JOURNAL OF SOLID STATE CHEMISTRY 43, 63–72 (1982)

New Phases in Equimolar $PbO-V_2O_5$ System

ELISABETTA BAIOCCHI, MARCO BETTINELLI, AND ANGELO MONTENERO*

Istituto di Chimica Fisica, Università di Parma, Parma, Italia

AND LORENZO DI SIPIO

Istituto di Chimica Generale ed Inorganica, Università di Padova, Padova, Italia

Received November 20, 1981

The quenching of the equimolar $PbO-V_2O_5$ melt gave rise to an amorphous material or two polycrystalline phases mixed with an amorphous matrix, depending on the cooling rate. These materials were submitted to heat treatment and all generated pure lead metavanadate crystals. All phases were characterized by means of powder X-ray diffraction, differential thermal analysis, scanning electron microscopy, and infrared absorption spectroscopy. Furthermore, the interdependence of all the amorphous and crystalline phases is explained. It was also possible to evaluate the kinetic parameters (activation energy and reaction order) of the glass → α-LPV phase transformation. It was confirmed that this reaction follows the Avrami–Erofe'ev equation.

Introduction

The commonly accepted phase diagram of the $PbO-V_2O_5$ system is still that formulated by Amadori in 1917 (*1*) (Fig. 1). The successive reexaminations of the system have substantially confirmed the correctness of Amadori's results, with some modifications in the PbO-rich region, because new compounds were discovered (*2, 3*). Particularly the central region has remained unchanged with the presence of the eutectic point at 50% mol V_2O_5. Viting and Golubkova claimed nonexistence of lead metavanadate as a compound on the basis of thermal analysis and microstructural methods (*4*). On the contrary, Saxena and Sharma (*5*) reported the formation of PbV_2O_6. In particular, by means of conductometric, pH-metric, and potentiometric titrations of $Pb(NO_3)_2$ with $NaVO_3$, they separated a powder whose formula was PbV_2O_6; their measurements were very accurate and reproducible. In addition, by slow cooling of a melt whose composition was $PbO : V_2O_5 = 1 : 1$, Jordan and Calvo (*6*) prepared single dark crystals, which were investigated by X-ray diffraction; the structural results allowed the authors to state that their compound was undoubtedly lead metavanadate. In order to confirm the stability of PbV_2O_6, they submitted it to a heat treatment and observed no variations in the structural arrangement of the sample.

From the aforementioned results some contradictions appear. It is evident that the structural and thermodynamic situation of the equimolar system is not clearly defined and that further investigations are needed.

Another source of interest regarding this

* To whom all correspondence should be addressed.

0022-4596/82/070063-10$02.00/0

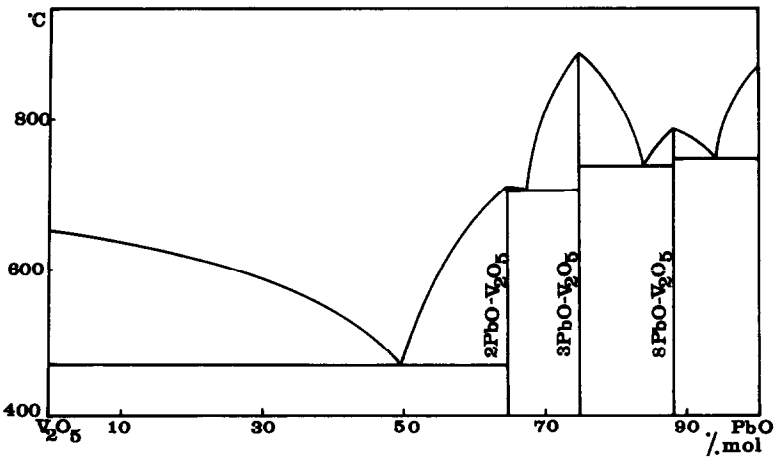

FIG. 1. Amadori's phase diagram of the $PbO-V_2O_5$ system.

system comes from the study of its glass-forming capability. In fact, there are only a few studies on glasses containing large amounts of V_2O_5 as unique network former (*7–10*), though the analogous systems containing P_2O_5 have been widely characterized since 1953 (*11–13*).

Experimental

Equal molar amounts of PbO and V_2O_5 were melted in an electrically heated muffle furnace under air atmosphere and at temperatures ranging from 700 to 1100°C. The total weight of the batch varied from 10 to 35 g. The melt was then quenched rapidly on materials with different thermal conductivity. This fact clearly influenced the cooling rate and in this way samples were obtained with different macroscopical appearance, glassy or polycrystalline, which were very dark brown in color. They were submitted to heat treatment at selected temperatures depending on the thermal analysis data. Powder X-ray diffraction (XRD) analysis was carried out on the prepared materials by using a Philips diffractometer with copper K_α radiation according to the Debye–Scherrer method. Because of the lack of literature data about lead vanadates, the experimental patterns were compared with the theoretical ones calculated with the aid of a computer. Microphotographs and point probe analysis of the different samples were performed by means of a Cambridge Stereoscan 250 scanning electron microscope equipped with an EDS Ortec microanalysis apparatus.

The thermal behavior of the samples was investigated by means of differential thermal analysis (DTA) carried out by a Linseis L62 thermoanalyzer in the 20–600°C range.

Infrared absorption spectra were recorded by a 283 Perkin–Elmer ir spectrophotometer. The samples were analyzed in the solid state after inclusion in KBr pellets.

Results and Discussion

No correlation was found between the macroscopical properties of the obtained materials and the melting temperature of the batch. On the contrary, as previously pointed out, we could obtain samples of different appearance by varying the quenching materials. In particular we used a stainless-steel hemispherical vessel, a copper plate, and a liquid nitrogen-cooled graphite vessel. Unlike the samples quenched on metal, which exhibited a poly-

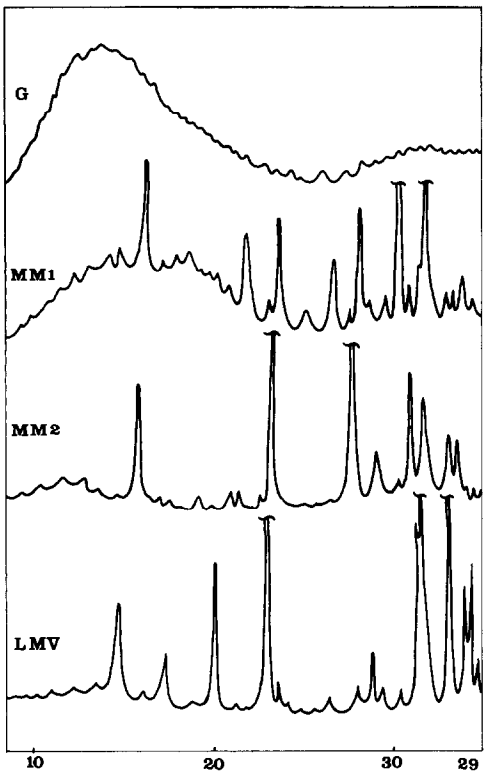

FIG. 2. X-Ray powder diffractograms of G, MM1, MM2, and LMV. G = glass; MM1 = quenched on copper; MM2 = quenched on stainless steel; LMV = lead metavanadate.

crystalline surface, the material obtained by using the graphite vessel had a glasslike lustrous look. Its XRD spectrum presented no peaks, but only a broad diffuse scattering at low angle and this is characteristic of a long-range structural disorder (Fig. 2).

The scanning electron microphotograph (Fig. 3) exhibited a surface without any presence of microstructures.

The DTA measurements displayed a typical glass pattern (Fig. 4), with a characteristic annealing dip, standing for the glass transition at 242°C, two exothermic peaks beginning at 245 and 379°C, and a sharp, intense endothermic one at 480°C. From the aforementioned data, we confirmed that the samples obtained by quenching on graphite were true glasses. We named these glasses as G. The chemical analysis, carried out by standard volumetric methods, showed that G had the same composition as the original batch.

The two series of samples quenched on the copper plate (named MM1) and on the stainless-steel vessel (named MM2) were submitted to XRD powder analysis. They gave different patterns where, besides the common broad diffuse scattering, several peaks stood out clearly coming from crystalline structures (Fig. 2). In these materials the presence of long order zones was also proved by SEM photographs, where needlelike crystals appeared mixed with an amorphous matrix, responsible for the low angle scattering (Figs. 5–7).

Though the XRD patterns belonged to two different crystalline structures, the EDS microanalysis showed that the crystalline phases in MM1 and MM2 had the same stoichiometry Pb : V = 1 : 1, which corresponds to the formula $Pb_2V_2O_7$, i.e., lead pyrovanadate, whereas the new amorphous matrix (G1) was richer in V_2O_5 than the batch, according to the ratio Pb : V = 1 : 2, 13. From the lever rule, the amount of the amorphous phase was 10.44 times greater than that of the lead pyrovanadate.

The only known structure of a compound having formula $Pb_2V_2O_7$ is that of chervetite (*14*). We simulated its XRD powder spectrum by a computer and compared the obtained pattern with the experimental ones. As the angle and the intensity of the peaks turned out very different, we concluded that the crystalline structures present in MM1 and MM2 belonged to two different unknown phases of $Pb_2V_2O_7$ which we called α-LPV and β-LPV. Attempts to interpret the diffraction patterns were made on the basis of the manual Ito's technique and were refined by the computerized least-squares method. Whereas no reliable results were obtained for the α-LPV phase because of its less-ordered structure, we calculated the cell parameters and indexed

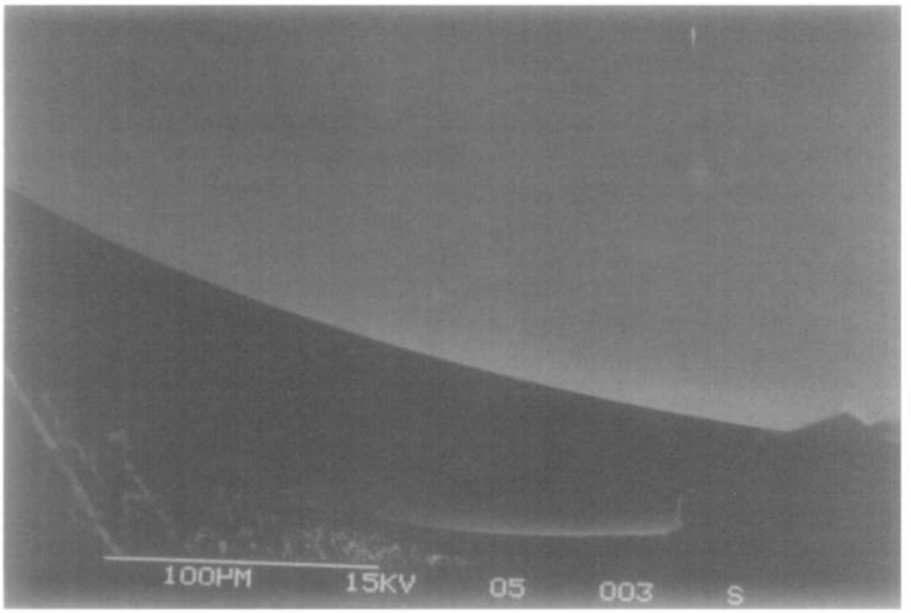

FIG. 3. SEM microphotograph of the amorphous phase G (×760).

the pattern of the β-LPV phase in triclinic symmetry (Table I); however, the obtained values are capable of improvement.

Besides G, MM1, and MM2 were also submitted to DTA analysis. All the samples exhibited the annealing dip at 242°C, indicating the presence of the amorphous phase and three peaks at the same temperatures as in G. By the usual technique of stopping the temperature rise and performing XRD powder analysis, we were able to understand the changes in our samples. In this way, we attributed the first exothermic peak present in the DTA pattern of G to the spontaneous transformation of a part of the amorphous phase into crystalline α-LPV. For what concerns MM1 and MM2 samples, the peak centered at about 298°C, more intense in the MM2 thermogram than in that of MM1, showed the transformation of a fraction of the amorphous phase into the crystalline phase which was already present in that sample, i.e., α-LPV in MM1 and β-LPV in MM2. This autocatalysis is known as "breeding" phenomenon. The

TABLE I

LATTICE PARAMETERS AND INDEXATION OF X-RAY POWDER DIFFRACTOGRAM OF β-LPV

a = 9.468 Å	α = 85.57°
b = 5.521 Å	β = 127.95°
c = 6.045 Å	γ = 97.93°
V = 246.780 Å^3	

ϑ	d_{obsd} (Å)	d_{calcd} (Å)	h	k	l	I_{obsd} (a.u.)
6.400	6.9103	6.8895	1	0	0	52
10.050	4.4140	4.3888	−2	0	1	100
12.200	3.6450	3.6368	−2	1	1	85
12.375	3.5943	3.5788	2	0	0	29
12.850	3.4635	3.4872	0	−1	1	29
12.875	3.4569	3.4557	0	1	1	29
13.875	3.2121	3.2038	−2	−1	1	57
14.050	3.1729	3.1499	−2	1	0	23
14.250	3.1293	3.1178	1	0	1	47
14.925	2.9908	3.0144	−3	0	1	33
15.200	2.9379	2.9279	−2	0	2	32
16.400	2.7282	2.7548	−1	0	2	34
16.800	2.6650	2.6652	−2	1	2	23
17.100	2.6196	2.6380	1	1	1	19
17.350	2.5830	2.6023	−1	2	0	14
18.550	2.4213	2.4176	3	0	0	27

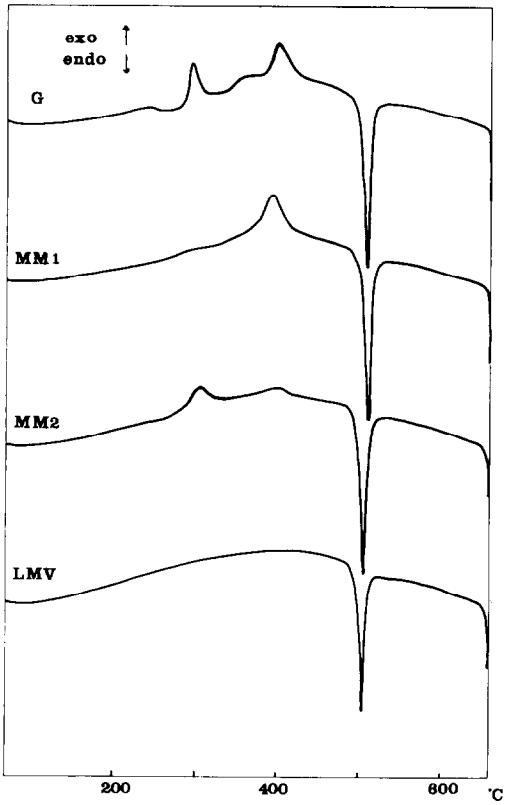

FIG. 4. Differential thermal analysis patterns of G, MM1, MM2, and LMV. Heating rate = 10°C/min.

common exothermic peak at 396°C is due to the formation of a homogeneous crystalline phase, which was identified as PbV_2O_6, lead metavanadate (LMV) (Fig. 8). Literature data (*15*) show that at about 500°C the melting of lead metavanadate occurs and this agrees with the endothermic peak observed in our patterns.

All the previous measurements clearly indicated that the phases are correlated with each other and that all converge to the formation of LMV. This trend showed that, besides G, the crystalline phases α-LPV and β-LPV are metastable and that the lead metavanadate should be the only thermodynamically stable compound in the investigated system. In order to verify this last assumption, we carried out DTA cooling runs on all the samples starting from the melt. In all the cases we observed only the same crystallization peak and the obtained material, analyzed by XRD technique, was found to be uniquely LMV. This agreed with the Jordan–Calvo preparation (*6*).

We can summarize the interdependence among the phases as in Fig. 9. Our results regarding the crystallization of the amorphous phase agree completely with those obtained by Dimitriev *et al.* (*16*).

We again point out that the fundamental step in the preparation of an amorphous or crystalline sample is the cooling rate, which is correlated with the thermal conductivity of the material used for the quenching, i.e.:

Material	Thermal conductivity (kcal sec · m · °C)
graphite	6.28
copper	1.70
stainless steel	0.08

As stated by Ostwald's step rule, when a metastable state "is spontaneously destroyed, the solid phase produced is not the most stable under the existing conditions, but the next in order" (*17*). In this respect, we recorded and interpreted the ir spectra of all the materials and this confirmed the previous statement. In fact ir vibrational spectroscopy supplies a reliable view of the internal structure of a compound. Though we were unable to surely assign the absorption bands, it was possible to give evidence of a continuous change in the pattern of the ir spectra, from the metastable glass G to the stable LMV passing through the two phases α-LPV and β-LPV (Fig. 10).

The low-energy spectrum of the glass G presented no peaks, but only a very broad band in the 1000- to 400-cm^{-1} region. This fact is strictly correlated with the high internal disorder. In the study of the spectra of MM1 and MM2 materials, we noted a more definite pattern due to the crystalline α-

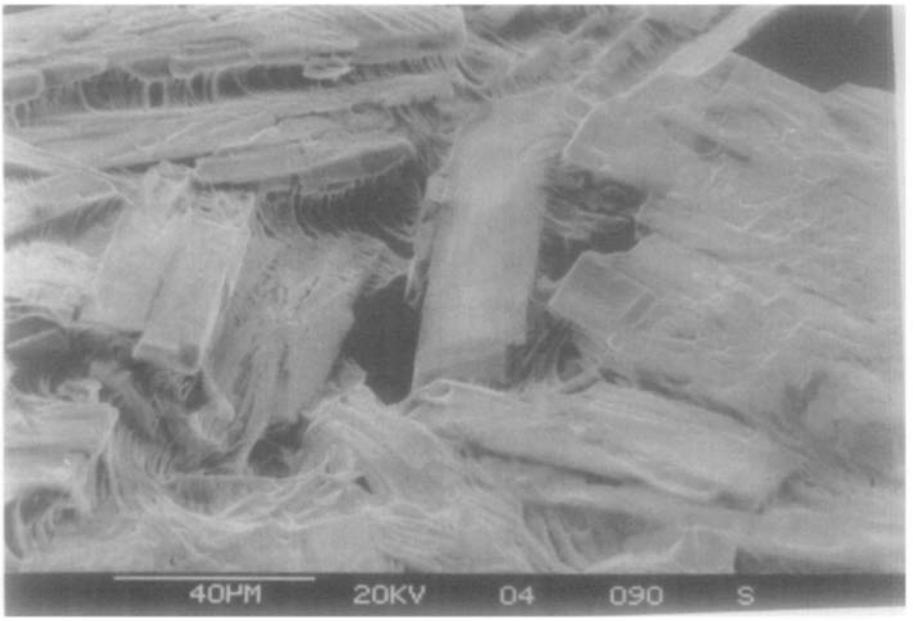

FIG. 5. SEM microphotograph of MM1 (×1400).

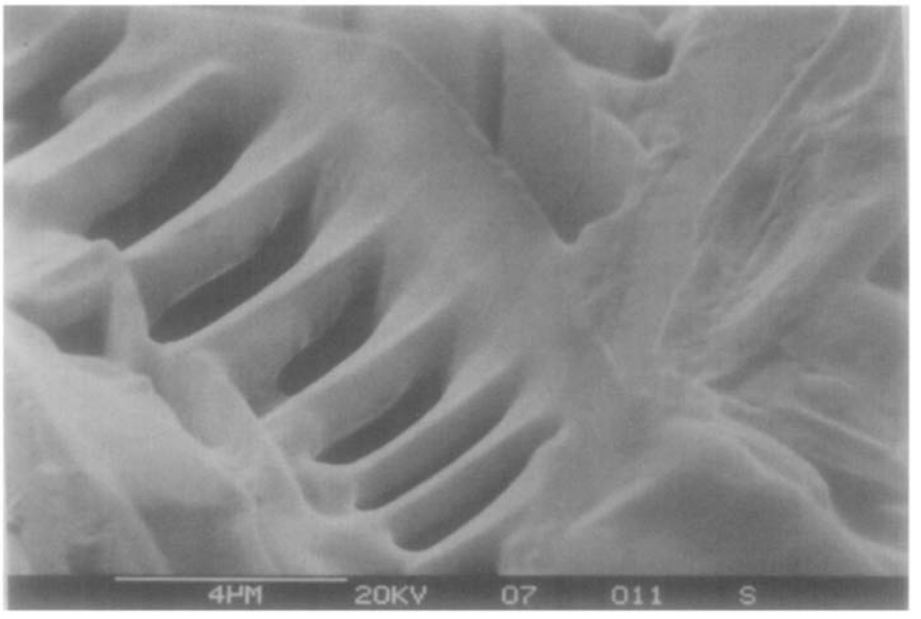

FIG. 6. SEM microphotograph of MM1: particular of the amorphous phase G1 (×16,000).

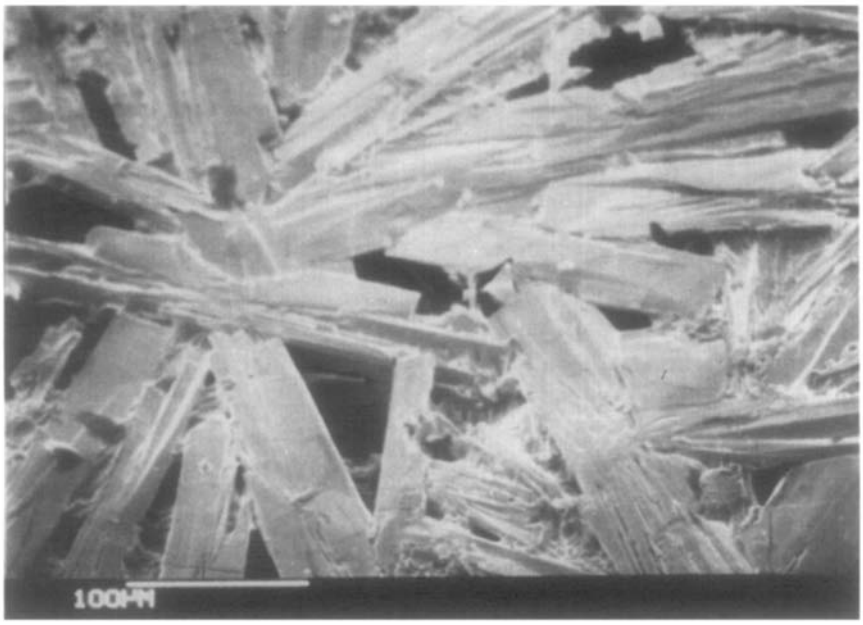

FIG. 7. SEM microphotograph of MM2 (×500).

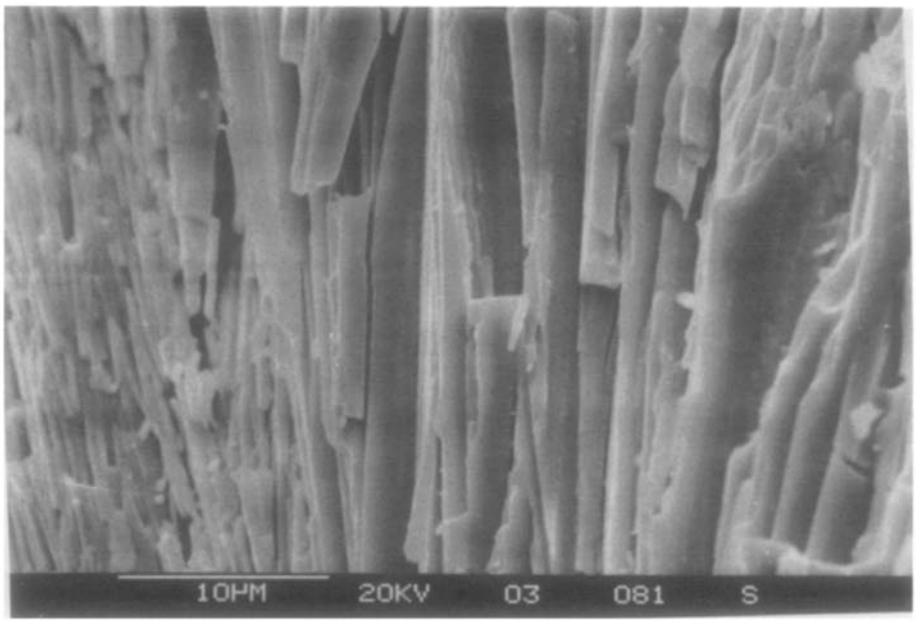

FIG. 8. SEM microphotograph of lead metavanadate (×5800).

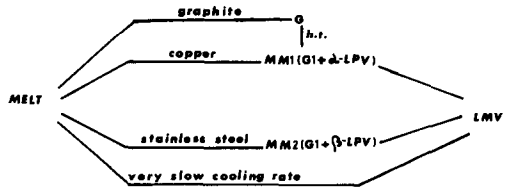

FIG. 9. Summary of the intercorrelations among G, MM1, MM2, and LMV.

LPV and β-LPV phases superimposed on a broad amorphous band. As expected, the LMV spectrum presented a well-defined series of narrow peaks without any contribution of the disordered phase. We noted that the β-LPV spectrum was more similar to the LMV one than that of the α-LPV phase, which resembled that of the amorphous phase. In this way the already discussed stability order G < α-LPV < LMV was again confirmed. By comparison with the known data, we found that the ir spectra concerning α-LPV and β-LPV were very different from that of chervetite (*18*), as was previously verified for the XRD data. On the basis of the work of Dupuis and Viltange (*19*) and Ross (*20*) we tentatively assigned the bands of α-LPV and β-LPV as shown in Table II.

In recent years several papers appeared which reported the use of DTA technique and which demonstrated that it is possible to determine the most important kinetic parameters of a crystallization process in an amorphous phase, such as the activation energy E_{act} and the reaction order n (*21–24*).

Among the crystallization reactions occurring in our system, the only one which we studied from a kinetic point of view was G → α-LPV. By assuming that this process is described by the Avrami–Erofe'ev equation (*25–28*), we submitted several amorphous samples to differential thermal analysis with different constant heating rates h (20, 10, 5, 2, 1 °C/min) in order to calculate E_{act} by means of the equation $\log h = -(E_{act}/4.57)\ (1/T) + \text{const}$ (Fig. 11). We calculated E_{act} = 74.8 kcal/mol, which was within the range of the known data for similar processes. The reaction order was evaluated by plotting $\log\Delta T$ versus $1/T$ accord-

TABLE II

INTERPRETATION OF THE ir ABSORPTION BANDS OF α-LPV AND β-LPV

Assignment	α-LPV (cm^{-1})	β-LPV (cm^{-1})
$\nu_s(VO_3)$	965 925	1005
$\nu_{as}(VO_3)$	870 820	865
ν_{as}(bridging OVO)	765	760
ν_s(bridging OVO)	535	580
$\delta(VO_3)$	435 340	340

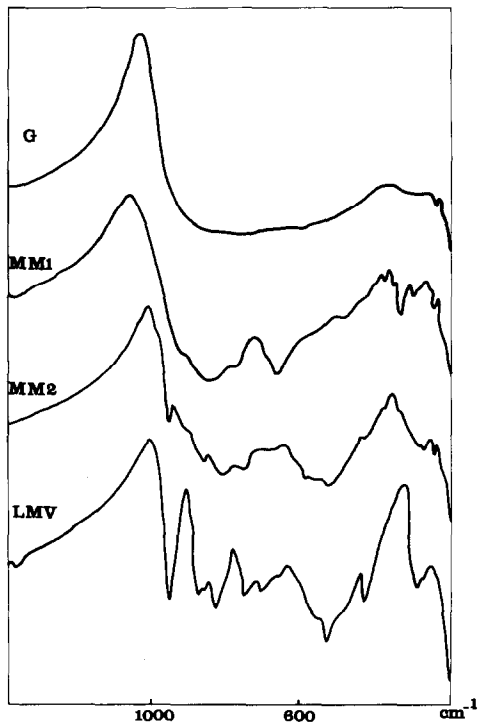

FIG. 10. Infrared absorption spectra of G, MM1, MM2, and LMV.

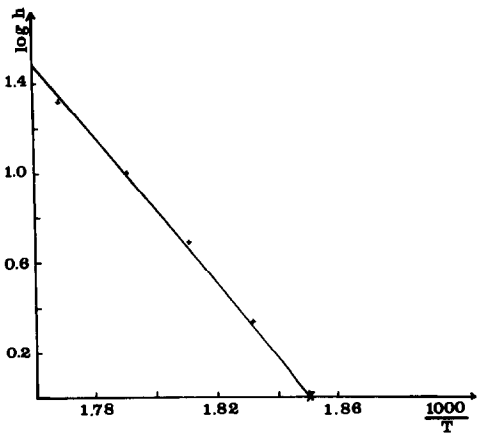

FIG. 11. Graphic evaluation of the activation energy of the G → Gl + α-LPV transformation by means of DTA measurements. Correlation coefficient = 0.9980.

ing to the relation $\log\Delta T = -(n E_{act}/4.57)(1/T) + \text{const}$ (*23*), where ΔT is the difference of temperature between the reacting compound and the reference material and T is the corresponding temperature of the reference (Fig. 12). The DTA pattern used for this determination was recorded at a 20°C/min heating rate. The obtained value n = 2.7 suggested that the crystallization reaction is controlled by diffusion and occurs with a constant nucleation rate and tridimensional growth.

Conclusions

The 50% mol $PbO-V_2O_5$ system forms a wide range of materials, all coming from the same melt. The determining reason for this behavior is surely the cooling rate which causes the formation of different compounds according to their thermodynamic stability and crystallization rate. The cooling rate can be controlled by choosing a quenching material with proper thermal conductivity. In the case of a graphite vessel, which exhibits the highest thermal conductivity, we have the formation of a true glass.

The α-LPV phase, which is dispersed in MM1, is found either by quenching on copper, which is the second material in thermal conductivity, or by heat treatment. Its ir spectrum shows that it has an internal structure similar to the glass one, though with a greater long-range order. All these facts, together with DTA results, suggest that α-LPV is a metastable phase intermediate between G and LMV.

The β-LPV phase is obtained only by quenching with a lower cooling rate with respect to α-LPV, whereas we could not observe the G → β-LPV and the α-LPV → β-LPV transformations by heat treatment. Though it has not been possible to determine an overall stability order, the preparation method indicates that β-LPV is formed by a path parallel to that of α-LPV, but characterized by a smaller crystallization rate, according to a more ordered structure rather similar to that of LMV, as shown by the ir spectra and by the XRD data.

Finally, all our experimental results agree on the conclusion that lead metavanadate can be prepared as a definite compound by slow cooling of a melt or by heat treatment of various metastable phases. Therefore, it seems very opportune to reexamine the $PbO-V_2O_5$ phase diagram, especially in the region nearby the eutectic point.

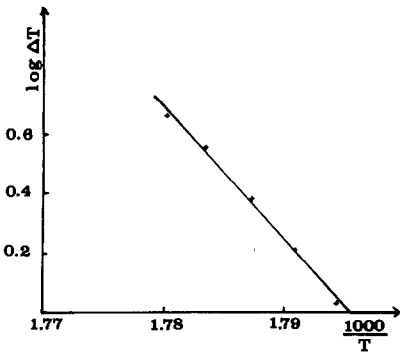

FIG. 12. Graphic evaluation of the reaction order of the G → Gl + α-LPV transformation by means of DTA measurements. Correlation coefficient = 0.9951.

Acknowledgments

We wish to thank Professor M. Nardelli, Head of the Istituto di Chimica Generale ed Inorganica of Parma University, for the use of the facilities in performing the XRD measurements. This work was financially supported by CNR (Italian National Research Council) in the Progetto Finalizzato per la Chimica Fine e Secondaria.

References

1. M. Amadori, *Atti R. Ist. Veneto Sci.* **76,** 419 (1917).
2. T. Shimoira, S. Iwai and H. Tagai, *J. Ceram. Assoc. Japan* **75,** 352 (1967).
3. J. Eckstein, K. Recker, and F. Wallrafen, *J. Cryst. Growth* **30,** 276 (1975).
4. L. M. Viting and G. P. Golubkova, *Vestn. Mosk. Univ. Ser. II: Khim.* **19,** 88 (1964).
5. R. S. Saxena and C. P. Sharma, *Bull. Chem. Soc. Japan* **41,** 377 (1968).
6. B. D. Jordan and C. Calvo, *Canad. J. Chem.* **52,** 2701 (1974).
7. Y. Kawamoto, M. Fukuzuka, Y. Ohta, and M. Imai, *Phys. Chem. Glasses* **20,** 54 (1979).
8. Y. Kawamoto, J. Tanida, H. Hamada, and H. Kiriyama, *J. Non-Cryst. Solids* **38–39,** 301 (1980).
9. V. H. Gahlmann and R. Brückner, *Glastech. Ber.* **50,** 104 (1977).
10. C. H. Chung and J. D. Mackenzie, *J. Non-Cryst. Solids* **42,** 357 (1980).
11. E. P. Denton, H. Rawson, and J. E. Stanworth, *Nature (London)* **173,** 1030 (1954).
12. G. N. Greaves, *J. Non-Cryst. Solids* **11,** 427 (1973).
13. Y. Limb and R. Davis, *J. Amer. Ceram. Soc.* **62,** 403 (1979).
14. A. Kawahara, *Bull. Soc. Fr. Mineral. Cristallogr.* **90,** 279 (1967).
15. Gmelin, *Handb. Anorg. Chem.* **570** V (B), 48 (1967).
16. Y. Dimitriev, I. Ivanova, and E. Gatev, *J. Non-Cryst. Solids* **45,** 297 (1981).
17. Quoted in M. Volmer, "Kinetics of Phase Formations," p. 7, Steinkopff, Dresden (1939).
18. "Sadtler Standard Spectra," published by Sadtler Research Laboratories, Philadelphia, Y 888 K.
19. T. Dupuis and M. Viltange, *Mikrochim. Ichnoanal. Acta,* 232 (1963).
20. S. D. Ross, "Inorganic Infrared and Raman Spectra," p. 276, McGraw–Hill, London/New York (1972).
21. J. Sestak, *Phys. Chem. Glasses* **15,** 137 (1974).
22. H. E. Kissinger, *Anal. Chem.* **29,** 1702 (1957).
23. A. Marotta and A. Buri, *Thermochim. Acta* **25,** 155 (1978).
24. K. Matusita and S. Sakka, *Thermochim. Acta* **33,** 351 (1979).
25. M. Avrami, *J. Chem. Phys.* **7,** 1103 (1939).
26. M. Avrami, *J. Chem. Phys.* **8,** 212 (1940).
27. M. Avrami, *J. Chem. Phys.* **9,** 177 (1941).
28. B. V. Erofe'ev, *C. R. Dokl. Acad. Sci. URSS* **52,** 511 (1946).